AGH DRILLING, OIL, GAS • Vol. 30 • No. 4 • 2013

http://dx.doi.org/10.7494/drill.2013.30.4.421

Tomasz Śliwa*, Łukasz Gałuszka**

STUDY OF THE EFFECT OF MEDIUM FLOW PARAMETERS ON HEAT TRANSFER IN THE LABORATORY COAXIAL MODEL OF A BOREHOLE HEAT EXCHANGER***

1. INTRODUCTION

Borehole heat exchangers (BHE) are more and more commonly applied for recovering energy from rock mass renewable sources and for rational heat managing in the heating/cooling installations. BHE exploitation simulations can be either provided by mathematic methods, included in examples [8, 9] or by carrying out tests at laboratory stands. BHEs located in the Laboratory of Geoenergetics in Faculty of Drilling, Oil and Gas AGH University of Science and Technology are being used to conduct research in area of presented interests [1].

A research on the efficiency of heat transfer in a coaxial borehole heat exchanger is described in this paper. In recent times theme of adapting old or not used anymore oil and gas wells is highly increased. The most important fact is that every deep well that is being transferred into BHE has to be of centric construction. This is for minimizing of pressure [7].

The objective of the study is to adjust the materials and the configuration of a vertical borehole heat exchanger in such a way that the heat transfer processes can be analyzed. A series of experimental measurements were performed for various capacities. Three various pipe materials were used in the experiments: polyethylene (PE), polyvinylchloride (PVC), polypropylene (PP) or a combination there of. The vertical borehole heat exchanger operated at the rock mass temperature. In laboratory conditions the rock mass heat source was substituted with 4 heating blankets, 80 W each. The polyethylene and polyvinylchloride pipes constituted flow channels in two zones. Their diameter differed depending on the applied combinations. The inner diameter of the heat exchanger equaled to 25.3 mm. The

* AGH University of Science and Technology, Faculty of Drilling, Oil and Gas, Department of Drilling and Geoengineering, Krakow, Poland.

** AGH University of Science and Technology, Student Scientific Association GEOWIERT, Krakow, Poland

*** The work was realized within the Statutory Research Program at the AGH UST Faculty of Drilling, Oil and Gas, AGH UST contract no. 11.11.190.555

experiments were carried out continuously: the process was monitored and measurement data collected. Each change in the flow intensity was related with the flow stabilization time. At least 30 measurements were made for each assumed volumetric flow of a heat carrier. Three temperature sensors were installed in the borehole heat exchanger; the flow was regulated with two valves.

The vertical borehole heat exchanger is usually used when the utility area is small and when higher and steady temperature of the rock mass is available. The efficiency of heat recovery is a function of supply temperature and flow losses, which causes the vertical borehole heat exchanger to bring about higher heat gains.

Due to the way in which they were performed, vertical borehole heat exchangers can be divided into [5]:
- U-type,
- concentric (Fig. 1).

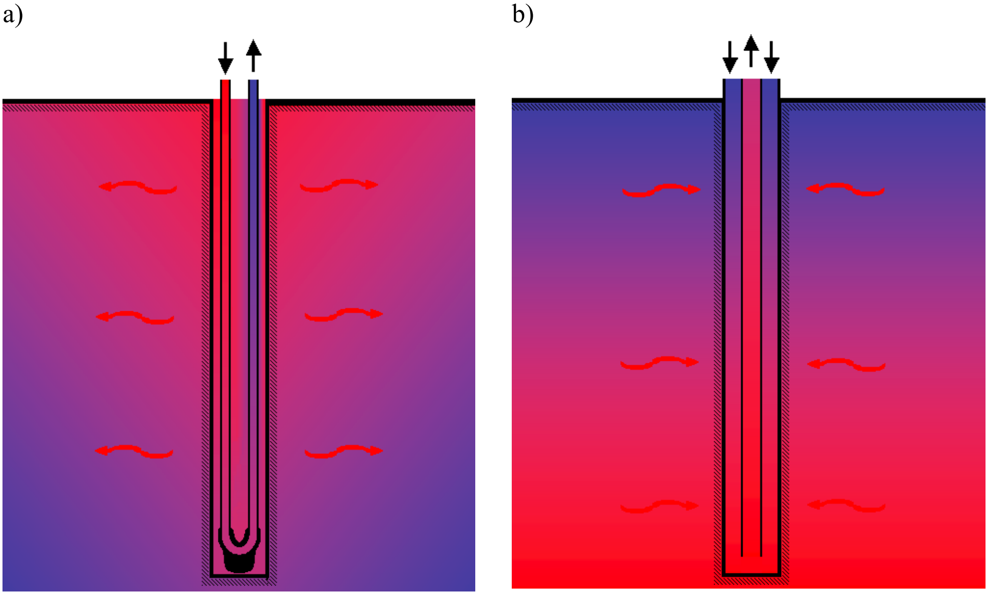

Fig. 1. Schematic of a U-type borehole heat exchanger (a) and coaxial (b) [6]

The measuring stand consists of three elements: vertical borehole heat exchanger (Fig. 2), measuring apparatuses (temperature sensors and flow meter shown in scheme on Figure 2) and a computer for recording results. The vertical borehole heat exchanger consists of an external layer, i.e. housing protecting it against mechanical damaging, and heating blankets at the steel pipe. The internal part of the laboratory model of the vertical borehole heat exchanger (steel pipe) has a 25.3 mm inner diameter and 2.15 meter lenght (Fig. 2). This was the place where various tube configurations were introduced for experimental purposes. Three temperature sensors were disposed at the BHE inlet and outlet, and one at its bottom.

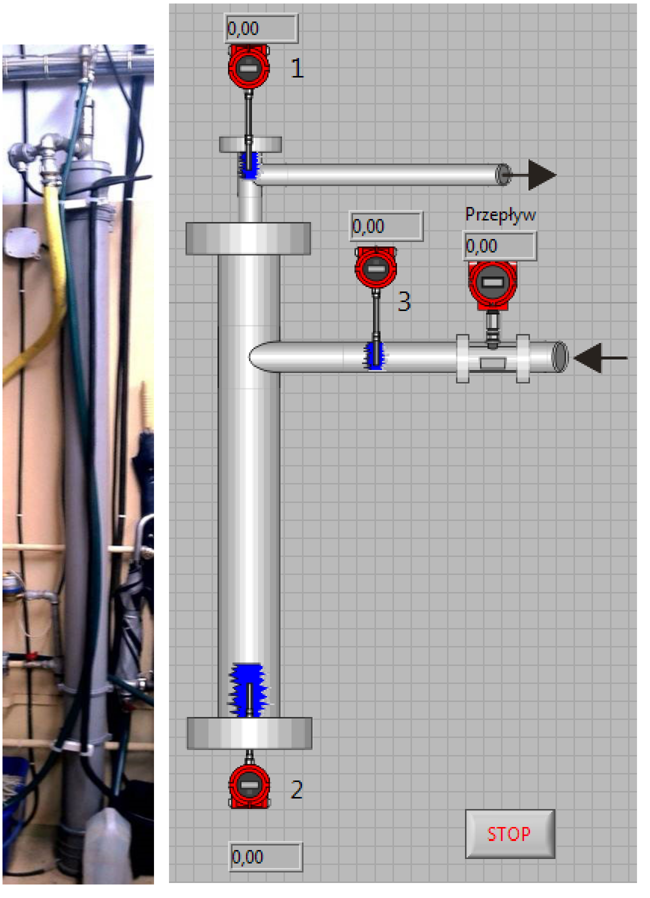

Fig. 2. Measuring stand – model of a vertical borehole heat exchanger and schematic of the stand: 1, 2, 3 – temperature sensors

2. CALCULATION ASSUMPTIONS

It is assumed that for Re < 2300 the flow is laminar, and for Re > 4000 the flow is turbulent [2]. Within the range of ⟨2300; 4000⟩ the flow is transitory. The Reynolds number can be calculated from the equation:

$$\mathrm{Re} = \frac{v \cdot d_h \cdot \rho}{\mu} \tag{1}$$

where:

v – average flow rate [m·s^{-1}],
d_h – hydraulic diameter [m],
μ – dynamic fluid viscosity coefficient [Pa·s],
ρ – fluid density [kg·m^{-3}].

The notion of hydraulic diameter is defined as a quotient of fourfold annular space to wetted perimeter, for annulus space it is:

$$d_h = D_{\text{in}} - d_{\text{out}} \tag{2}$$

where:

D_{in} – internal diameter of a well (outside pipe) [m],
d_{out} – outside diameter of internal column (inside pipe) [m].

Amount of heat provided by the borehole heat exchanger is calculated from the equation:

$$Q = \dot{V} \cdot \rho \cdot c_w \cdot \left| T_{\text{in}} - T_{\text{out}} \right| \tag{3}$$

where:

$\dot{V}$ – flow rate of fluid in the model of borehole heat exchanger [$m^3 \cdot s^{-1}$],
ρ – density of fluid (heat carrier) [$kg \cdot m^{-3}$],
c_w – specific heat of fluid flowing through the borehole heat exchanger [$J \cdot kg^{-1} \cdot K^{-1}$],
T_{in} – temperature of inflowing heat carrier [K],
T_{out} – outflow temperature of a carrier flowing through the borehole heat exchanger [K].

3. CALCULATION METHODICS

Initially, the analyzed pipes (inner column) are calculated for flow conditions so that a turbulent or transitional flow is obtained in the annular space between the pipe and the borehole heat exchanger's wall, and laminar flow inside the pipe (the lower range of flow intensity). The upper range is obtained when a turbulent flow is obtained inside the pipe.

Measurements are performed for the obtained ranges as to obtain at least a 6-grade range of flow intensity changes. A heat flow vs. flow intensity curve is plotted on the basis of the obtained results (Fig. 5).

Calculation assumptions were made for the research. They resulted from the design of the borehole heat exchanger, way in which the experiment was performed and the applied medium (network, tap water) with the temperature 15°C:

- specific heat of water $c_w = 4186\ J \cdot kg^{-1} \cdot K^{-1}$,
- kinematic viscosity $\eta = 1.14 \cdot 10^{-6}\ m^2 \cdot s^{-1}$,
- water density $\rho = 999.2\ kg \cdot m^{-3}$.

Flow intensity was analyzed for the 0 to 10 liters per minute for points, where the flow was steady and even. Properties of materials used for performing insulating column in the borehole heat exchanger's model are listed in Table 1.

Table 1

Material of inner column data (according to its construction showed in Table 2)

Material	Density [$kg \cdot m^{-3}$]	Heat conductivity [$W \cdot m^{-1} \cdot K^{-1}$]
PVC	1390	0.16
PR	920	0.22
PE	960	0.42
water	1000	0.58

The design of a internal columns are presented in Figure 3 and Table 2. Configuration A and B are based on a two-pipe inner column, whereas configuration C is a single-pipe construction.

Table 2

Design of a laboratory model of a borehole heat exchanger – three configurations (d_o, d_i – outer and inner diameters, respectively, b – wall thickness)

Column of pipes	Configuration A	Configuration B	Configuration C
Outer layer	Steel pipe, D_{out} = 25.3 mm		
First layer	Flow channel in annular space		
Second layer	PE pipe d_o = 25.0 mm, b = 2.0 mm	PP pipe d_o = 22.0 mm, b = 3.0 mm	PP pipe d_o = 22.0 mm, b = 3.4 mm
Third layer	Water	Microfracture	–
Fourth layer	PE pipe d_o = 20.0 mm, b = 2.0 mm	PVC pipe d_o = 16.0 mm, b = 1.0 mm	–
Inside	d_i = 16.0 mm	d_i = 14.0 mm	d_i = 15.2 mm

a) b) c)

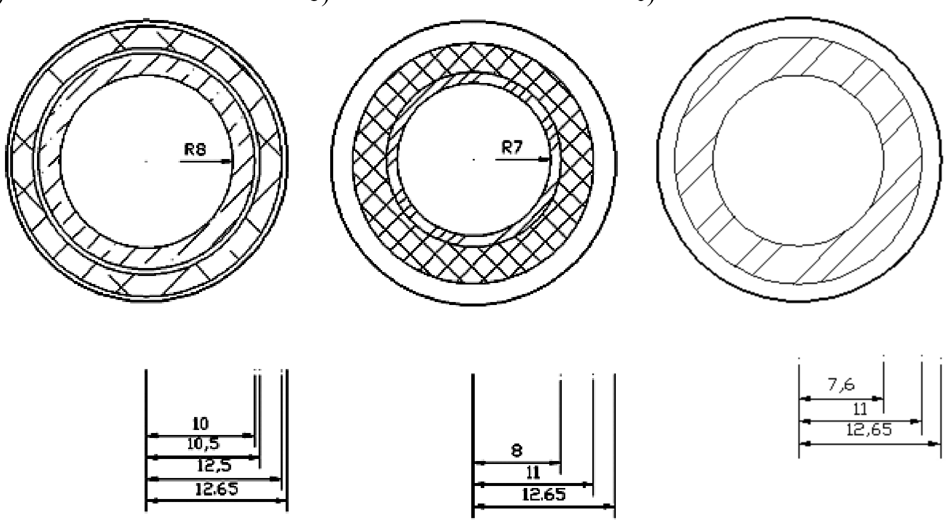

Fig. 3. Structure of inner column: a) configuration A (two PE pipes); b) configuration B (PP and PVT pipe); c) configuration C (single PP pipe)

The characteristic of analyzed flows is shown in Tables 3–5. The average flow rate and the Reynolds number were determined based on the volume flow rate of the heat carrier.

Tabela 3

Calculation of flow conditions for given capacities, accounting for inner space and annular space of a vertical borehole heat exchanger – design A (area of annular space cross section equals to 11.85 mm^2, and of inner space 201.06 mm^2)

Volume of heat flow [$dm^3 \cdot min^{-1}$]	Rate of the carrier in annular space [$m \cdot s^{-1}$]	Rate of the carrier inside the column [$m \cdot s^{-1}$]	Re number in annular space [–]	Re number inside the column [–]
0.29	0.352	0.021	82	258
0.50	0.703	0.041	164	516
0.80	1.125	0.066	263	825
1.20	1.688	0.099	394	1238
1.60	2.250	0.133	525	1650
2.10	2.813	0.166	656	2063
2.60	3.656	0.216	853	2682
3.40	4.781	0.282	1116	3507
4.41	6.328	0.373	1477	4642
5.10	7.313	0.431	1706	5364
5.75	7.875	0.464	1838	5777
6.40	9.000	0.531	2100	6602
7.11	9.985	0.589	2330	7324
7.80	10.969	0.647	2559	8046
8.61	12.094	0.713	2822	8871
9.50	13.360	0.787	3117	9800

Table 4

Calculation of flow conditions for given capacities, accounting for inner space and annular space of a vertical borehole heat exchanger – design B (area of annular space cross section equals 122.59 mm^2, and of inner space 153.94 mm^2)

Volume of heat flow [$dm^3 \cdot min^{-1}$]	Rate of the carrier in annular space [$m \cdot s^{-1}$]	Rate of the carrier inside the column [$m \cdot s^{-1}$]	Re number in annular space [–]	Re number inside the column [–]
0.40	0.054	0.043	140	472
0.70	0.095	0.058	244	632
1.20	0.163	0.099	419	1083
1.80	0.245	0.149	628	1625
2.57	0.340	0.207	872	2257
2.77	0.394	0.240	1012	2618
3.34	0.462	0.282	1186	3069
3.90	0.530	0.323	1361	3520
4.19	0.598	0.365	1535	3972
5.38	0.734	0.448	1884	4874
6.30	0.870	0.531	2233	5777
7.63	1.033	0.630	2652	6860
9.14	1.224	0.746	3140	8124
9.78	1.305	0.796	3350	8665

Table 5

Calculation of flow conditions for given capacities, accounting for inner space and annular space of a vertical borehole heat exchanger – design C (area of annular space cross section equals to 122.59 mm^2, and of inner space 181.46 mm^2)

Volume of heat flow [$dm^3 \cdot min^{-1}$]	Rate of the carrier in annular space [$m \cdot s^{-1}$]	Rate of the carrier inside the column [$m \cdot s^{-1}$]	Re number in annular space [–]	Re number inside the column [–]
0.38	0.054	0.037	140	434
0.6	0.082	0.055	209	652
1.10	0.150	0.101	384	1194
1.65	0.218	0.147	558	1737
2.20	0.299	0.202	768	2389
2.77	0.381	0.257	977	3040
3.40	0.476	0.321	1221	3800
4.19	0.571	0.386	1466	4561
5.20	0.707	0.478	1814	5646
5.80	0.789	0.533	2024	6298
6.30	0.843	0.569	2163	6732
7.40	1.020	0.689	2617	8144
8.41	1.142	0.772	2931	9121
9.62	1.305	0.882	3350	10424

4. RESULTS OF THE MEASUREMENTS

Figure 4 contains the results of temperature measurements (ΔT) received by the heat carrier. The dependence of heating capacity on the volume of the heat carrier flow rate is presented in Figure 5. The heat capacity increase is observed only for the initial values of the heat carrier flow rate. At higher values the capacity is even (stable) regardless of the type of insulating column.

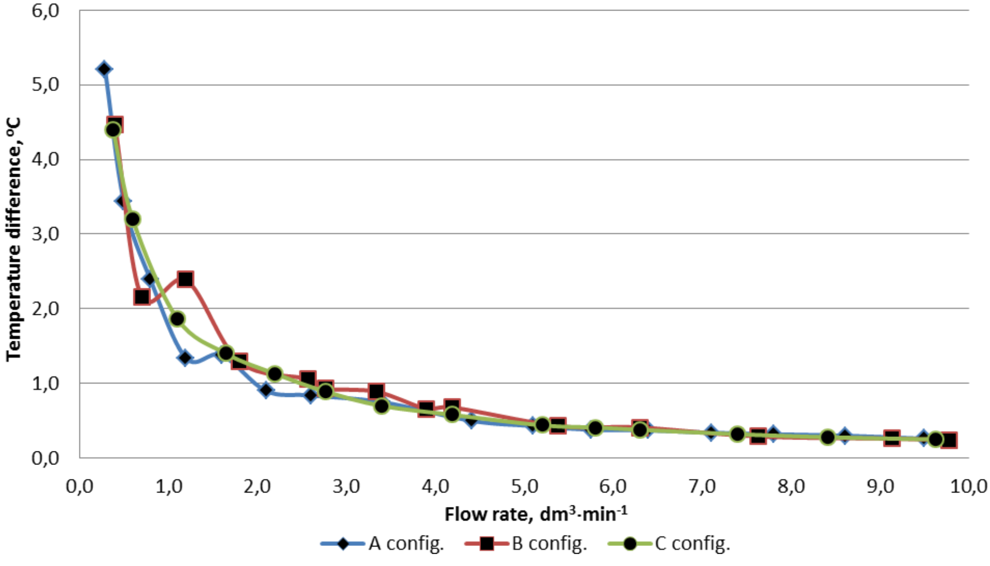

Fig. 4. Dependence of temperature difference of the heat carrier volume flow rate for all laboratory BHEs design models

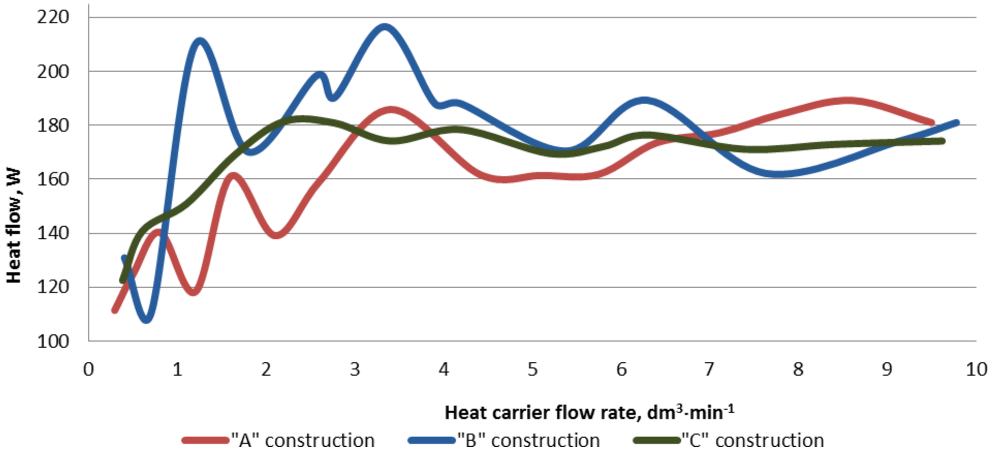

Fig. 5. Dependence of heat flow transmitted from the heat carrier volume for all laboratory BHEs design models

The energy efficiency peak for each conducted configuration is located in a transitory flow regime. The transfer into the turbulent flow resulted in lower values for the heating power. The instability in heat stream provided by laminar flow shows us that the flow regime is not suited to exploitation regime projects of BHEs.

Owing to the character of the experiment we can assume that for each volume rate a steady state was obtained for heat flow through the barrier in vertical borehole heat exchanger designs. For a few cylindrical layers differing in thickness and conductivity, the following calculations can be made [2–4]:

$$Q = 1{,}163 \cdot \frac{\left(T_{p(1)} - T_{p(n+1)}\right)}{\sum_{i=1}^{n}\left(\frac{1}{\lambda_i}\frac{d_i}{F_{mi}}\right)} \tag{4}$$

where:

Q – heat rate [W],
F_{mi} – surface area of the layer [m^2],
$T_{p(1)}$ – temperature on the exterior layer [K],
$T_{p(n+1)}$ – temperature of layer closer to center [K],
λ_i – material thermal conductivity [W·m^{-1}·K^{-1}],

By transforming equation (4) we can calculate the successive temperatures at the border of particular configurations. With the obtained results we can establish the course of heat flow through the barrier.

5. CONCLUSIONS

1. Three various designs of insulating pipes were analyzed in a laboratory model of a concentric borehole heat exchanger. Experiments were performed for the heat carrier flow rates from 0.2 dm^3·min^{-1} to almost 10 dm^3·min^{-1}.
2. Figure 5 represents a dependence on heating capacity obtained in the BHE on the heat carrier flow rate. The capacity increase was observed only for the initial range of heat carrier flow rates. Optimum, taking into consideration each configuration of BHE was around capacity 3.3–3.5 dm^3·m^{-1}. Increasing flow rate results in higher pressure losses, without income in the efficiency of the heat stream (Fig. 5). At higher values of the capacity was observed that the heating power is not being more effective, no matter the type of insulating column used.
3. In configuration B, where PP and PVC pipes were used, the value of nearly 220 W was obtained, at the flow rate 3.4 dm^3·min^{-1}. For configuration C, the heat transfer reached a maximal level at a flow rate of 2.2 dm^3·min^{-1}. At the higher flow rate values the system turned out to be most steady. In each configuration capacity equals or higher than 3.6 dm^3·min^{-1} is represented by a turbulent flow regime. Therefore optimization is expected before or at the beginning of the turbulent state, which was proven by the conducted experiment.
4. Configuration A of BHE provides a free space between the pipes. This space is filled with water. Despite such design, no heat exchange typical of counterflow was observed.

5. More experiments should be performed using various materials to determine the optimal configuration. Materials used in BHEs should not be the only aim for next research. An important aspect in the area of heat transfer efficiency is also the flow rate in regards to power transmitted to the BHEs from surroundings.
6. The measurement series consisted of 30 measurements made for each steady flow intensity. The normal distribution of results stayed within the range one standard deviation proving a high accuracy of equipment used in and the stability of the process itself.

REFERENCES

[1] Gonet A., Śliwa T.: *Otworowe wymienniki ciepła jako źródło ciepła lub chłodu na przykładzie Laboratorium Geoenergetyki WWNiG AGH.* Wiertnictwo, Nafta, Gaz t. 28, z. 1–2, 2011, pp. 419–429.

[2] Hobler T.: *Ruch ciepła i wymienniki*. Wydawnictwo Naukowa-Techniczne, Warszawa 1971.

[3] Jaafar A., Escudier M.P., Poole R.J.: *Transition to turbulence in a concentric annular pipe*. The 6th Annual European Rheology Conference, 7–9 April 2010, Sweden, pp. 99–102.

[4] Pudlik W.: *Wymiana i wymienniki ciepła.* Wyd. Politechniki Gdańskiej, Gdańsk 1988.

[5] Śliwa T.: *Otworowe wymienniki ciepła: prace geoinżynieryjne w pozyskiwaniu i magazynowaniu ciepła* [*Borehole heat exchangers: geoengineering in heat extraction and storage*]. Nowoczesne Budownictwo Inżynieryjne: Inżynieria Sanitarna, Geoinżynieria, Tunelowanie, Górnictwo, Hydrotechnika, Drogi, Mosty, nr 3, 2005, pp. 42–44.

[6] Śliwa T., Gonet A., Złotkowski A.: *Górotwór jako magazyn ciepła. Możliwości magazynowania i pozyskiwania ciepła za pośrednictwem otworowych wymienników ciepła* [*Rockmass as heat reservoir*]. Nowoczesne Budownictwo Inżynieryjne: Inżynieria Sanitarna, Geoinżynieria, Tunelowanie, Górnictwo, Hydrotechnika, Drogi, Mosty, nr 6, 2007, pp. 12–14.

[7] Śliwa T., Kotyza J.: *Application of existing wells as ground heat source for heat pumps in Poland.* Applied Energy, vol. 74, 2003, pp. 3–8.

[8] Śliwa T., Gonet A.: *Theoretical model of borehole heat exchanger*. Journal of Energy Resources Technology, vol. 127, no. 2, 2005, pp. 142–148.

[9] Śliwa T., Gołaś A., Wołoszyn J., Gonet A.: *Numerical model of borehole heat exchanger in ANSYS CFX software*. Archives of Mining Sciences, vol. 57, no. 2, 2012, pp. 375–390.